

Numerical Simulation of Heat Transfer in Turbulent Pipe Flow with Structured Wall Surfaces

Peter Renze

Institute of Energy and Drive Technology
University of Applied Sciences Ulm
Germany
renze@hs-ulm.de

Abstract— Innovative heat transfer technology is the key to the optimization of many processes in the power or process industry. Operational costs and usage of valuable resources can be reduced, if the heat transfer efficiency is increased and pressure loss is reduced. Therefore, the current work is focused on heat transfer enhancement at tubes with micro-structured walls with turbulent flow. In this kind of geometry modern optical measurement technology cannot be applied and the analysis of the turbulent transport is only possible with numerical flow simulations. A large-eddy turbulence model is applied to account for turbulence closures. First, the simulation setup is validated with data from the literature and then several micro-structured geometries are investigated. The simulations are computationally costly and depend on high performance computing (HPC). The open-source software library OpenFOAM® is applied to perform massively parallel simulations.

Keywords—computational fluid dynamics; heat transfer enhancement; turbulence; micro-structured tubes

I. INTRODUCTION

Modern high performance heat exchangers are of great importance in many industrial applications like power generation, cooling, refrigeration, chemical processes and other production processes. In these industries the necessity to increase production at lower consumption of resources is a demanding task. Optimizing heat transfer equipment is a crucial part in the overall process optimization. Therefore, innovative heat transfer technologies are required.

The term *heat transfer enhancement* is used in the literature to describe the improvement of the heat transfer coefficient k . Thus, the heat transfer is increased or the heat transfer area can be reduced while keeping the heat transfer rate constant. Either way, the efficiency of the process is increased. This is a classical challenge for the engineering and many researches have published on this topic, see [1, 2].

In the scope of this paper the heat transfer enhancement at tubes with micro-structured wall surfaces are investigated at turbulent flow conditions. Numerical flow and heat transfer simulations are performed using the open-source software library OpenFOAM® in massively parallel simulations.

II. METHODS

A. OpenFOAM

OpenFOAM® (Open Source Field Operation and Manipulation) is an object-oriented software library programmed in C++ and designed for the numerical solution of differential equation from continuum mechanics, see Jasak and Weller [3]. The main usage is in the area of computational fluid mechanics. OpenFOAM® was declared open-source in 2004 and is distributed free of charge. It is licensed under the GPL, which makes it ideal for simulations in the area of academic as well as industrial research.

OpenFOAM® is distributed with a variety of pre-designed solvers. Usually the finite volume method (FVM) is applied, but there are applications of the finite-element method (FEM) available as well. New solvers and algorithms can be easily generated by adaption and combination of available physical model implementations. These are structured in the form of object oriented classes, e.g. within the turbulence class several approaches are available like Reynolds-averaged-Navier-Stokes (RANS), large-eddy simulation (LES), or direct numerical simulation (DNS) as well as hybrid approaches.

The top-level structure of OpenFOAM® makes it easy for engineering students or unexperienced programmers to begin the design of their own code. The strictly object-oriented programming of OpenFOAM® puts a strong focus on objects instead of functions. The pre-processing is done classically via the command line terminal, but in the online community a large

number of scripts or graphical user interfaces (GUI) are available today. The computational meshes can be generated within the software, they are unstructured and based on hex-dominant cells. For graphical post-processing of the simulation results integrated modules in ParaView [4] are provided.

B. Physical Modeling

The physical modeling of flows with heat transfer is based on conservation laws for mass, momentum, and energy. The continuity equation for an unsteady flow of a compressible fluid can be formulated as

$$\frac{\partial \rho}{\partial t} + \nabla \cdot (\rho \mathbf{u}), \quad (1)$$

with the nabla operator ∇ , the density ρ , and the vector of velocity \mathbf{u} . Thus, the conservation of momentum is formulated

$$\frac{\partial(\rho \mathbf{u})}{\partial t} + \nabla \cdot (\rho \mathbf{u} \mathbf{u}) = -\nabla p + \rho \mathbf{g} + \nabla \cdot (2\mu_{eff} \mathbf{S}(\mathbf{u})) - \nabla \cdot \left(\frac{2}{3} \mu_{eff} (\nabla \cdot \mathbf{u}) \right), \quad (2)$$

where p is the static pressure, \mathbf{g} the constant of gravity, and μ_{eff} is the sum of the molecular and turbulent dynamic viscosity. The deformation tensor $\mathbf{S}(\mathbf{u})$ is defined as $\mathbf{S}(\mathbf{u}) = \frac{1}{2} (\nabla \mathbf{u} + (\nabla \cdot \mathbf{u}) \mathbf{T})$.

The conservation of energy is formulated using the variable of inner energy e

$$\frac{\partial(\rho e)}{\partial t} + \nabla \cdot (\rho \mathbf{u} e) + \frac{\partial(\rho k)}{\partial t} + \nabla \cdot (\rho \mathbf{u} k) + \nabla \cdot (p \mathbf{u}) = \nabla \cdot (\alpha_{eff} \nabla e) + \rho \mathbf{u} \cdot \mathbf{g}, \quad (3)$$

where $k = |\mathbf{u}|^2/2$ is the kinetic energy per mass unit. The effective thermal diffusivity α_{eff} is defined as

$$\alpha_{eff} = \frac{\rho v_t}{Pr_t} + \frac{\mu}{Pr} = \frac{\rho v_t}{Pr_t} + \frac{\lambda}{c_p} \quad (4)$$

where λ is the thermal conductivity, c_p the heat capacity at constant pressure, Pr_t is the turbulent Prandtl number and v_t the turbulent kinematic viscosity. The turbulent transport parameters in the equations (1) to (4) require a turbulence closure with a corresponding modeling technique.

In the literature, an isotropic concept for the turbulent Prandtl-number is pre-dominantly found, but recently tensor-based models are applied more often. A thorough discussion is not possible here, but recent improvement has been made in RANS-development like the v2-f-model [5, 6] or the scale-adaptive model [7]. In recent years the effort for the development of RANS-models has been strongly reduced due to lack of general success as well as the rapidly increasing computational resources that allow the application of more costly methods.

Here, the LES technique is applied, i.e. only the large-scale vortices that contain most of the turbulent kinetic energy are directly resolved and all smaller scale vortices are modeled [8, 9, 10]. Like this, the accuracy compared to RANS is increased substantially and at the same time the numerical effort compared to DNS is reduced up to a level that makes this approach interesting for the industry. A detailed overview about the LES techniques is given in [11]. These techniques have been demonstrated to perform well for technically relevant turbulent flows [12, 13, 14] and even for multiphase flows [15, 16, 17].

In LES a filter function with a characteristic filter width Δ is applied to equation (1)-(3), so that the field variables are decomposed into a resolved and a non-resolved part. Thus, the velocity vector becomes $\mathbf{u} = \hat{\mathbf{u}} + \mathbf{u}'$. The expression for the effective viscosity is reformulated to $\mu_{eff} = \mu + \mu_{SGS}$, i.e. the sum of molecular and apparent viscosity of the subgrid scales. Following the Boussinesq approximation the subgrid scale viscosity is then modeled as $\mu_{SGS} = \rho C_k \Delta \sqrt{k_{SGS}}$ with $C_k = 0.07$ and k_{SGS} as kinetic energy of the subgrid scales. The Smagorinsky model [8] is chosen with

$$k_{SGS} = \frac{C_k}{C_\epsilon} \Delta^2 |\mathbf{S}|^2 \quad (5)$$

with $C_\epsilon = 1.048$ and $|\mathbf{S}| = (\mathbf{S} : \mathbf{S})^{\frac{1}{2}}$.

In the current work an additional transport equation model for the kinetic energy is solved for some cases and the increased numerical effort will be juxtaposed to the gained accuracy. The equation reads

$$\frac{\partial k_{SGS}}{\partial t} + \nabla \cdot (k_{SGS} \mathbf{u}) - \nabla \cdot \left(\frac{\mu_{eff}}{\rho} \nabla k_{SGS} \right) = 2\nu_{SGS} |\mathbf{S}|^2 - \frac{C_\epsilon k_{SGS}^{\frac{3}{2}}}{\Delta}. \quad (6)$$

TABLE I. INFORMATION ABOUT HPC RUNS

HPC Details	Simulation Cases		
	<i>Smooth Tubes (outer forced convection)</i> <i>Re_D=6900, Pr=7</i>	<i>Smooth tubes (inside flow)</i> <i>Re_τ=180-314, Pr=7</i>	<i>Structured Tubes (inside Flow)</i> <i>Re_τ=180, Pr=7</i>
Execution time	96	144	192
Simulated time	10 flow cycles	10 flow cycles	10 flow cycles
Cores/Nodes	56 / 2	56 / 2	56 / 2
Number of time steps	~100000	~110000	~130000
Cell number	~8 millions	~8 millions	~26 millions

III. COMPUTATIONAL DETAILS

Most of the simulations have been performed within the scope of the bwHPC-C5 project using the bwUniCluster. Selected costly computations have been performed at the forHLR II cluster, where access has been granted to the author. More detailed information about the HPC runs are given in Table I.

IV. RESULTS

In this chapter the preliminary results of an ongoing project are presented. Before the heat transfer enhancement at tubes is investigated, the simulation setup as well as workflow are validated and the results are compared with literature.

A. Simulation of heat transfer at the turbulent flow around tubes

In Fig. 1 a visualization of the instantaneous flow and temperature field at forced convection around single tubes is given. The Reynolds number is calculated with the outer tube diameter and with the outer flow velocity u_D . It yields $Re_D = \frac{\rho u_D D}{\mu} = 6900$.

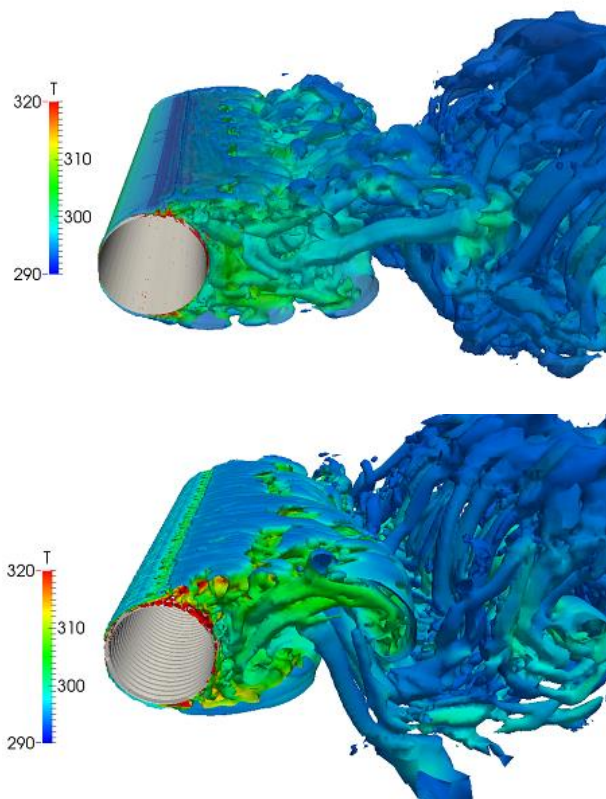


Fig. 1. Results of a large-eddy simulation (LES) of turbulent flow around tubes at $Re_D = 6900$ with a smooth heat transfer surface (top) and micro-structures (bottom).

Here, a constant wall temperature is applied as a boundary condition and the heat transfer to the fluid is calculated. In Fig. 1 (top) the coherent flow structures in this turbulent flow with periodic separation are emphasized using the Lambda2 method.

In Fig. 1 (bottom) the results of the simulation with identical setup but a different wall structure are presented. Here, the outer tube surface is micro-structured with fins. The separation phenomena are clearly effected as well as the heat transfer. The time averaged heat transfer is enhanced by around 20%. The variation of the heat transfer with time is about 10%

B. Simulation of heat transfer at turbulent pipe flow

The accurate calculation of heat transfer at the turbulent flow inside of tubes with a large-eddy simulation technique requires a far more complex numerical setup compared to the work in the previous section. The main challenge is the generation of turbulent inflow data at the inlet section of the pipe. Usually, the computational costs do not allow for the simulation of long pipe sections with a fully developed flow. That is why, only a small section is simulated, i.e. about 12 inner tube diameters.

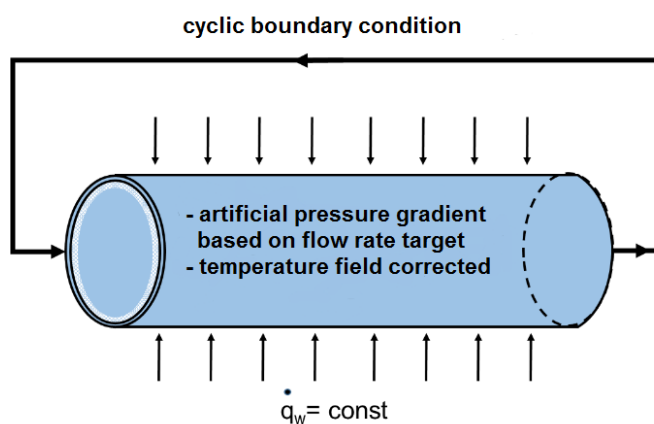


Fig. 2: Sketch of the numerical setup and the boundary condition for the LES of the turbulent flow through tubes.

Thus, at the flow inlet of the domain unsteady flow data has to be generated artificially. Assuming a fully developed turbulent flow field this can be done by applying cyclic boundary conditions between inlet and outlet. The pressure gradient that drives the flow is artificially introduced to the momentum equations. The numerical setup is shown in Fig. 2. The heat flux through the tube wall is usually defined by either a constant temperature or a constant heat transfer boundary condition at the wall surface depending on the validation case. In both cases the temperature data has to be corrected by the introduced heat flux if a cyclic boundary between inlet and outlet is used.

The computational meshes for all cases are generated with the grid generation tool *snappyHexMesh* distributed with OpenFOAM®. A sufficient wall resolution of around $y_+ = 0.1$ is reached by the application of prism layers near the wall. The unstructured meshes are predominantly cubical without stretching which results in a large number of total grid cells compared to literature cases. For the low Reynolds number cases this number is about 6 million. For most literature cases structured meshes with high grid stretching reduces the size of the mesh by a factor of up to 10. But with the current automated mesh generation setup complex wall surface structures can be meshed, which is a great advantage. Like this exactly the same setup can be used to simulate varying surface geometries eliminating the influence of mesh topology substantially.

In Fig. 3 snapshots of the 3D flow field of the simulations with a smooth tube surface are shown at an arbitrary time step. The coherent vertical structures (top) in the flow field and the instantaneous thermal boundary layer (bottom) are clearly visible.

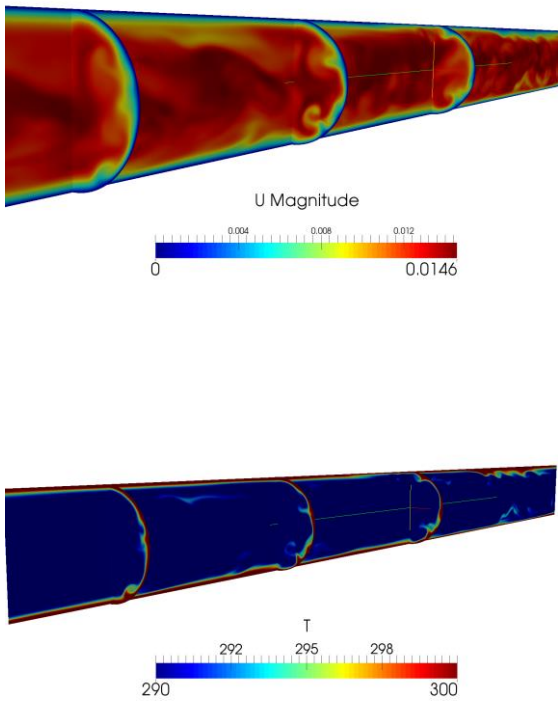


Fig. 3. Contours of the flow and temperature field at an instantaneous time step at a smooth tube surface, $Re_\tau = 180$, $Pr = 7$; top: magnitude of velocity; bottom: temperature.

Time averaged results of the simulations are shown in Fig. 4. The flow field has been averaged over 20 flow cycles. The velocity profile in radial direction that is shown in Fig. 4 has

been spatially averaged as well as time averaged. The velocity profile is shown in the classical logarithmic scale for two different Reynolds numbers, $Re_\tau = 180$ and $Re_\tau = 314$. The results match literature data very well considering the aforementioned design of the computational mesh.

An analysis of the heat transfer process is given in Table II. For the case of $Pr = 7$ and two Reynolds numbers the resulting Nusselt numbers are calculated from the simulations and compared with classical engineering correlations for heat transfer in turbulent pipe flow, see Gnielinski [18]. The results match very well and the simulation workflow proves to be capable of predicting turbulent heat transfer inside of tubes with reasonable accuracy.

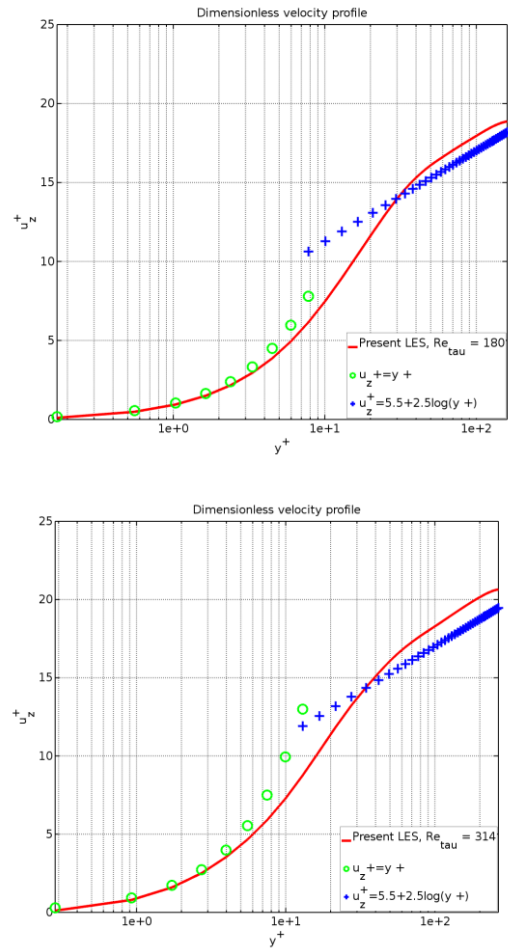


Fig 4. $Re_\tau = 180$, $Pr = 7$ (top), $Re_\tau = 314$, $Pr = 7$ (bottom)

TABLE II: Comparison of the simulated heat transfer (Nusselt number Nu) with literature data from Gnielinski [18]

Case	$Nu_{\text{simulated}}$	$Nu_{\text{literature}}$
$Re_\tau = 180$, $Pr = 7$	45.2	48.8
$Re_\tau = 314$, $Pr = 7$	86.9	81.7

In Fig. 5 preliminary results are shown for a simulation of turbulent flow inside of tubes with micro-structured surfaces at $Re_\tau = 180$. The computational mesh has been generated with exactly the same setup as described above. The increased complexity of the near wall mesh leads to a total number of 30 million grid cells. The transport processes will be analyzed in the ongoing work.

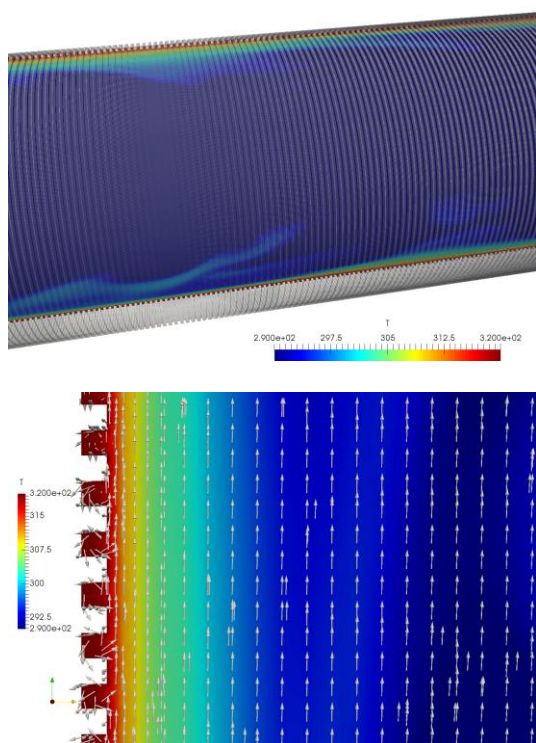


Fig. 5. Preliminary results of turbulent heat transfer through tubes with micro-structured surfaces at $Re_\tau = 180$, $Pr = 7$

V. SUMMARY

The software library OpenFOAM[®] is increasingly used for computational fluid dynamics in academic and industrial research. Here, it is applied to calculate the heat transfer enhancement by micro-structured surfaces in turbulent flows. The numerical setup has been validated by comparison of the results with literature data. Especially, the simulation of turbulent heat transfer inside of tubes is an intricate task. The current methods based on OpenFOAM[®] proved to be capable for this challenge. Preliminary results of simulations with complex surfaces have been shown. The physics of heat transfer enhancement will be thoroughly analyzed with the help of these methods in the scope of the ongoing work. So far it can be concluded, that the method can be readily applied to develop new surface structures for heat transfer enhancement. The numerical costs are not prohibitive and a later transfer of the method into the industry seems feasible.

ACKNOWLEDGMENT

The author likes to gratefully acknowledge the Steinbuch Center for Computing (SCC) at the Karlsruhe Institute of Technology (KIT) for the provided computational resources and support [19].

Nomenclature

ρ	density
\mathbf{u}	velocity vector
μ	dynamic viscosity
k	turbulent kinetic energy
\mathbf{S}	shear rate tensor
g	gravity constant
p	static pressure
α	heat transfer coefficient
λ	thermal conductivity
e	specific energy
Re_τ	Reynolds number based on friction velocity
Pr	Prandtl number or turbulent Prandtl number with subscript t

REFERENCES

- [1] A. E. Bergles, M. K. Jensen, B. Shome, Bibliography on Enhancement of Convective Heat and Mass Transfer. Heat Transfer Laboratory Report No HTL-23 Rensselaer Polytechnic Institute, 1995.
- [2] R. L. Webb, N. H. Kim, Principle of enhanced heat transfer. 2nd Edition. Taylor Francis: New York, NY, USA, 2005.
- [3] H. Jasak H., H.G. Weller, Interface tracking capabilities of the InterGamma differencing scheme, Technical Report, Imperial College, University of London, 1995.
- [4] J. Ahrens, B. Geveci, C. Law, ParaView: An End-User Tool for Large Data Visualization, Visualization Handbook, Elsevier, 2005, ISBN-13: 978-0123875822.
- [5] Laurence, D.R., Uribe J.C., Utyuzhnikov, S.V. A Robust Formulation of the v2-f Model, Flow Turbulence and Combustion, 73, 169-185, 2004.
- [6] Popovac, M., Hanjalic, K., Compound Wall Treatment for RANS Computations of Complex Turbulent Flows ans Heat Transfer, Flow Turbulence and Combustion, Nr. 78, S. 177-202, 2007.
- [7] Menter, F. R., and Y. Egorov. The scale-adaptive simulation method for unsteady turbulent flow predictions. Part 1: theory and model description. Flow, Turbulence and Combustion 85.1 (2010): 113-138.
- [8] J. Smagorinsky. General circulation experiments with the primitive equations, part I: The basic experiment. Monthly Weather Review, 91:99-164, 1963.
- [9] Germano, M., Piomelli, U., Moin, P. and Cabot, W. H. (1991), A dynamic sub-grid scale eddy viscosity model, Physics of Fluids, A(3): pp 1760-1765, 1991.
- [10] You, D. and Moin, P. (2007), A dynamic global-coefficient subgrid-scale eddy-viscosity model for large-eddy simulation in complex geometries, Physics of Fluids, 19(6): 065110, 2007.
- [11] Sagaut, Pierre (2006). Large Eddy Simulation for Incompressible Flows (Third ed.). Springer. ISBN 3-540-26344-6.
- [12] P. Renze, W. Schröder, M. Meinke, Large-eddy simulation of film cooling flows at density gradients, International Journal of Heat and Fluid Flow 29.1; 18-34, 2009.

- [13] P. Renze, W. Schröder, M. Meinke, Large-eddy simulation of film cooling flows with variable density jets, *Flow, Turbulence and Combustion* 80.1 (2008): 119-132, 2008.
- [14] P. Renze, W. Schröder, M. Meinke, Large-eddy simulation of film cooling flow ejected in a shallow cavity, *AIAA Paper* 927, 2007.
- [15] P. Renze, K. Heinen, M. Schönherr. Experimental and Numerical Investigation of Pressure Swirl Atomizers. *Chem Eng Tech*, 34 (7):1191–1198, 2011.
- [16] P. Renze, A. Buffo, D. L. Marchisio, M. Vanni, Simulation of Coalescence, Breakup, and Mass Transfer in Polydisperse Multiphase Flows, *Chemie Ingenieur Technik*, 86(7):1088–1098, 2014.
- [17] A. Buffo, D. L. Marchisio, M Vanni, P. Renze, Simulation of polydisperse multiphase systems using population balances and example application to bubbly flows, *Chem. Eng. Res. Des.*, 91(10):1859–1875, 2013.
- [18] Verein Deutscher Ingenieure, VDI-Gesellschaft Verfahrenstechnik und Chemieingenieurwesen (GVC). *VDI-Wärmeatlas: Berechnungsblätter für den Wärmeübergang*. 11. Auflage, 2013.
- [19] Steinbuch Center for Computing. *Forschungshochleistungsrechner ForHLR 2*. <http://www.scc.kit.edu/dienste/forh2r2.php>,